TRANSONIC FLUTTER WIND TUNNEL TESTS OF CONVENTIONAL TWIN-ENGINE TRANSPORT SEMISPAN MODEL

Hitoshi Arizono, Kazuyuki Nakakita, Jiro Nakamichi
***Japan Aerospace Exploration Agency**

Keywords: *Flutter, Transonic flow, Wind tunnel test*

Abstract

Transonic flutter wind tunnel tests with a twin-engine transport semispan model were conducted at Japan Aerospace Exploration Agency (JAXA). The test results would be used for understanding of the aeroelastic characteristics and for verifying simulation codes. The wind tunnel tests were conducted with the two configurations; the one has the wing with engine nacelle model and the other has the wing without engine nacelle model. The flutter mode of the wing with engine nacelle was coupled between the wing bending mode and the nacelle pitching mode, and the flutter mode of the wing without engine nacelle model was uncoupled between the wing bending mode and the wing in-plane bending mode. In this paper, the summary of the flutter tests is reported.

1 Introduction

The evaluation of the aeroelastic characteristics play a significant role in the structural design of an aircraft. In particular, it is difficult for a complicated configuration to estimate the aeroelastic characteristics precisely. In the transonic region, the nonlinear aerodynamic characteristics like shock waves make the phenomenon more complex.

Hong,et al [1], show the aeroelastic simulations and flutter boundary predictions with CFL3D and Reduced Order Modeling (ROM) technique on a twin-engine transport flutter model in the Transonic Dynamics Tunnel. The results of the simulations show good correlations to the experimental flutter hump mode, however, the flutter tip mode was over predicted by as much as 25%.

In the WIONA (Wing with Oscillating Nacelle) project with DLR and ONERA, interference effect between an unswept superciritical airfoil model and an annular wing representing an engine nacelle were investigated [2, 3].

The authors developed the aeroelastic simulation codes based on Euler equations, and verified using the wind tunnel tests of the wing-pylon-nacelle configuration. The estimated flutter boundary using the nonlinear simulations was about 10% higher than the results of the wind tunnel tests [4].

This present study reports results from experiments on the aeroelastic characteristics of the twin-engine transport at the transonic flow conditions. The wind tunnel test was conducted to investigate the aeroelastic characteristics of the twin-engine transport aircraft and to obtain the validation data for CFD simulation.

2 Wind Tunnel Test Setup

2.1 Wind Tunnel

The tests were conducted in the Transonic Flutter Wind tunnel at JAXA. This facility is mainly used for the research of transonic flutter. The wind tunnel layout is shown in Fig. 1. It is a typical blow down type of wind tunnel. The test section is 0.6 m $\times$ 0.6 m. Pressurized air (20 atm) is accu-

mulated in the vessels located outside which supplies air to the wind tunnel. A variety of flow conditions can be realized by controlling the mass flow with valves and vanes at the entrance of the flow channel. The used air is decelerated through the silencer and exhausted to the open air. The duration time of the operation is about 60 seconds. When flutter occurs, the flutter model is taken out of the wind tunnel to maintain it safe.

The operation range is 140 kPa – 400 kPa and 0.6 – 1.2, with respect to the total pressure and Mach number, respectively. Not only total pressure but also Mach number can be swept independently or keeping a linear relation between each other during a blow which lasts about 30 – 60 seconds. The present flutter wind tunnel tests were conducted in a range of Mach numbers 0.70 – 0.90, and total pressures, 150 kPa – 300 kPa.

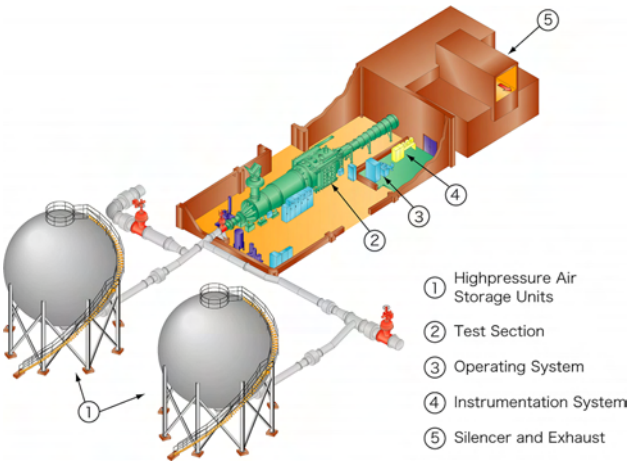

Fig. 1 Wind tunnel

2.2 Wind Tunnel Model

The research model is the conventional twin engine commercial jet aircraft, which consists of the wing-pylon nacelle model and the rigid fuselage-like fairing mounted on the wind tunnel wall. Fig. 2 shows the planform geometry of the semispan wind tunnel model. The wing section is a supercritical airfoil. The leading edge sweepback angle of the wing is 20.7 degee. The root chord length is 95.9 mm, the tip chord length is 25.3 mm and the span is the 270 mm. The dihedral angle of the wing is 6 degree. The engine nacelle which is the flow-through nacelle is mounted at 30% span station.

Both the stiffness and the mass distributions of the model are designed to generate a wing-nacelle flutter, which is important for the engine-wing-mounted aircraft, in the operating range of the wind tunnel. The main structure of the wing model consists of the aluminum beam to simulate the wing elastic properties and the aluminum rib-web plates to form the model into the aerodynamic shape with balsa. The pylon-nacelle model consists of the aluminum main structure and the plastic pylon-nacelle model fabricated with rapid-prototyping. The rigid fuselage-like fairing is designed and fabricated for use with the wing model which shifted the model away from the wind tunnel wall boundary layer while serving as an appropriate aerodynamic boundary condition at the wing root.

Five strain gauges are installed to measure the vibration of the wing and nacelle, which are located at the wing root, 70% span station and the pylon, respectively.

The wind tunnel tests were conducted using two configurations. the wing with the engine nacelle and without that. In order to identify the modal characteristics of the wind tunnel model, the impact hammer testing and the vibration analysis using MSC/NASTRAN were conducted. Tables 1 and 2 and Fig. 3 and 4 show the natural frequencies and the natural mode shapes of each configuration.

Fig. 5 and 6 show the results of the flutter analysis using MSC/NASTRAN at Mach number $M = 0.80$ for each model. The flutter speeds are 271 m/sEAS and 302 m/sEAS, respectively.

3 Result

For the above configurationse, the data were acquired for Mach numbers from 0.70 to 0.87 and for total pressures $P_0 = 150$ to 300 kPa. Angle of attack was varied from 0.0 to +1.0 degrees.

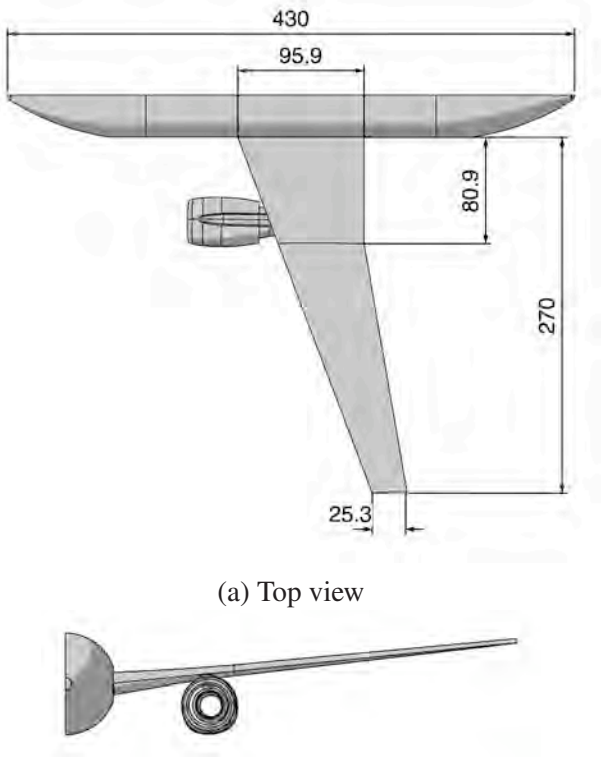

(a) Top view

(b) Front view

Fig. 2 Wind tunnel model

Table 1 Natural frequencies of the wing with engine nacelle model

#	Mode description	GVT (Hz)	NASTRAN (Hz)
1	1st wing bending	50.0	48.7
2	1st in-plane bending	130.0	130.7
3	nacelle pitching	132.5	133.9
4	nacelle rolling	157.5	155.7
5	2nd wing bending	197.5	193.6
6	nacelle yawing	–	304.5
7	3rd wing bending	427.5	419.4
8	2nd in-plane bending	471.3	496.8
9	1st wing torsion	–	497.9

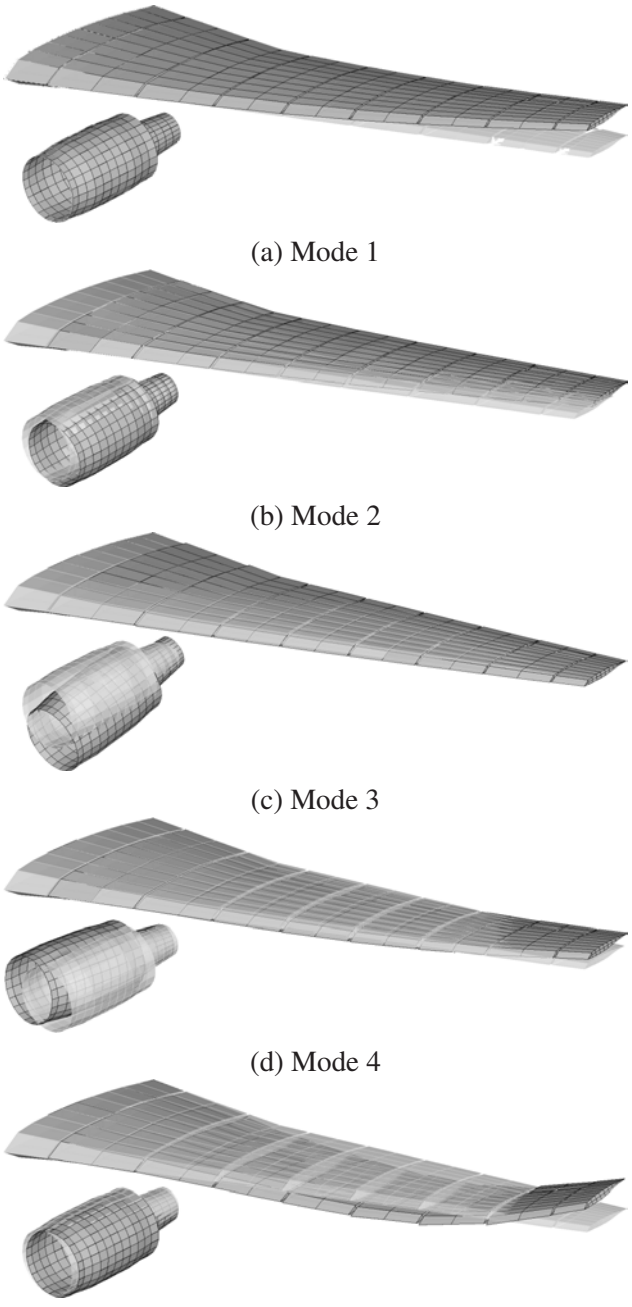

(a) Mode 1

(b) Mode 2

(c) Mode 3

(d) Mode 4

(e) Mode 5

Fig. 3 Mode shape of the wing with engine nacelle model

Table 2 Natural frequencies of the wing without engine nacelle model

#	Mode description	GVT (Hz)	NASTRAN (Hz)
1	1st wing bending	50.0	48.7
2	1st in-plane bending	132.0	132.7
3	2nd wing bending	196.0	191.8
4	3rd wing bending	444.0	432.4
5	1st wing torsion	470.0	491.6
6	2nd in-plane bending	518.0	506.2
7	4th wing bending	742.0	725.0
8	2nd wing torsion	806.0	865.0

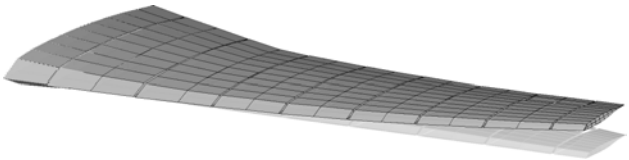

(a) Mode 1

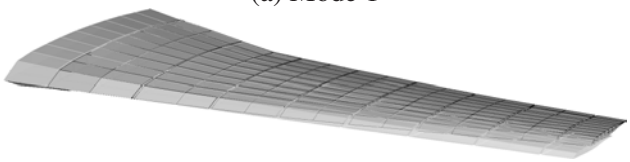

(b) Mode 2

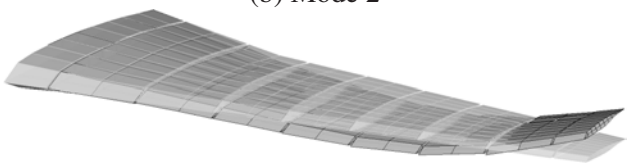

(c) Mode 3

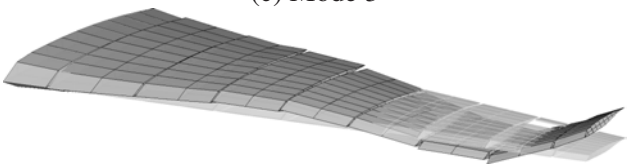

(d) Mode 4

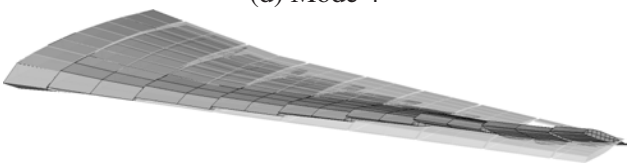

(e) Mode 5

Fig. 4 Mode shapes of the wing without engine nacelle model

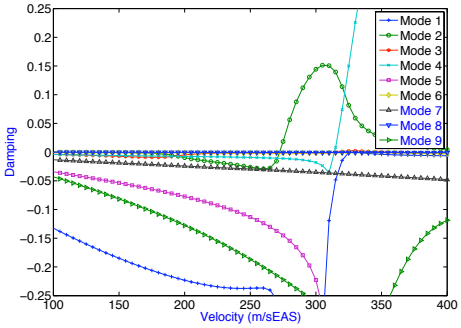

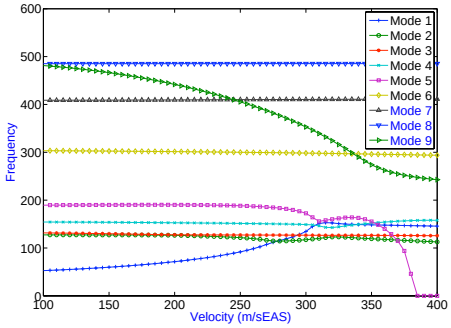

Fig. 5 $V-g$ plot for the wing with engine nacelle model ($M = 0.80$)

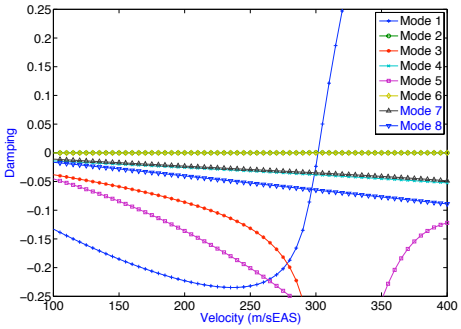

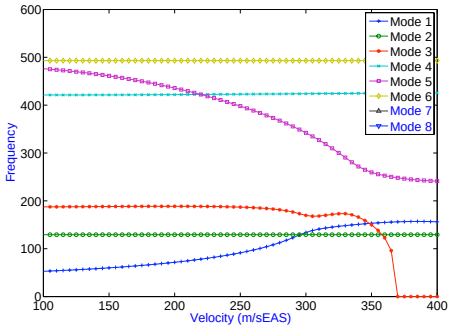

Fig. 6 $V-g$ plot for the wing without engine nacelle model ($M = 0.80$)

3.1 Wing with Engine Nacelle Model

Fig. 7 contains the time histories of the outputs of the strain gauges, the frequencies of the wing bending and torsion, and the phase difference between the wing bending and torsion.

The strain gauge outputs of the wing root torsion and the nacelle pitching have synchronized and these amplitudes have increased slowly with an increase in the velocity. The results show the frequency and the phase difference between the inboard wing bending motion and the inboard wing torsional motion are equivalent after time $t = 25$ sec. For that reason, the flutter mode is coupled between the wing 1st bending mode and the nacelle pitching mode. The flutter frequency is the 107 Hz. Fig.8 shows the image of CCD camera. The strong washout for the static aeroelastic deformation is observed during test because this model is not jig shape.

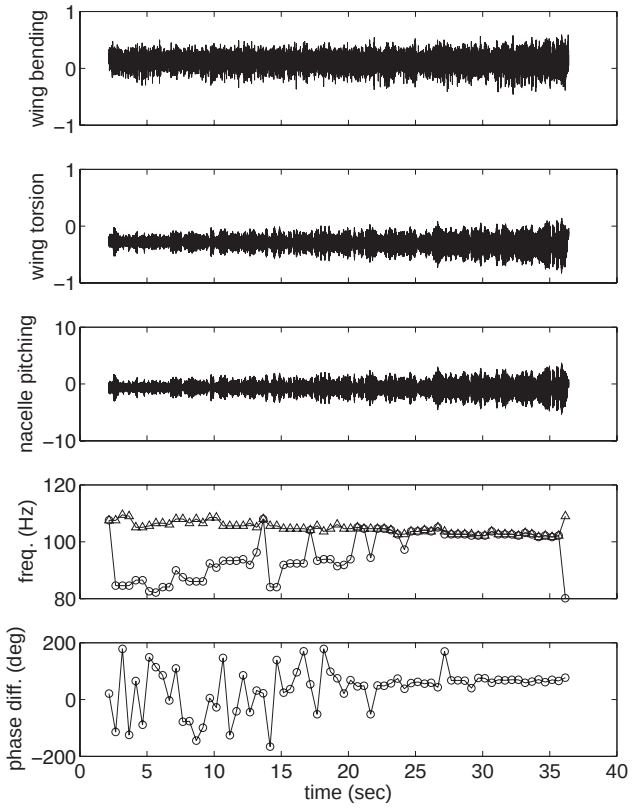

Fig. 7 Time history of strain gauge outputs, frequencies and phase difference of wing bending and torsion ($M = 0.82/P_0 = 150 - (1$ kPa/s$) - 200$ kPa$/V = 270 - 295$ m/sEAS$/$AoA $= +1$ degree)

3.2 Wing without Engine Nacelle Model

Fig.9 also show the time histories.

These results show that the frequency and the phase difference between the inboard bending motion and the inboard torsional motion are not equivalent. Fig. 10 shows the image of CCD camera. From the image of camera, the dominant vibration modes are the wing 1st bending mode, wing 2nd bending mode and wing 1st in-plane bending mode. The phase difference between these three mode is not constant.

It is difficult to estimate the in-plane mode flutter, because the estimated NASTRAN analysis is the hard flutter at 302 m/sEAS.

Fig. 8 Image of CCD camera (the wing with engine nacelle model)

4 Conclusion

The flutter wind tunnel tests were conducted in the transonic region using the conventional twin-jet transport semispan model. The flutter results has been obtained for two configurations which are the wing with and without engine nacelle model. These results are useful as the validation data for CFD simulation.

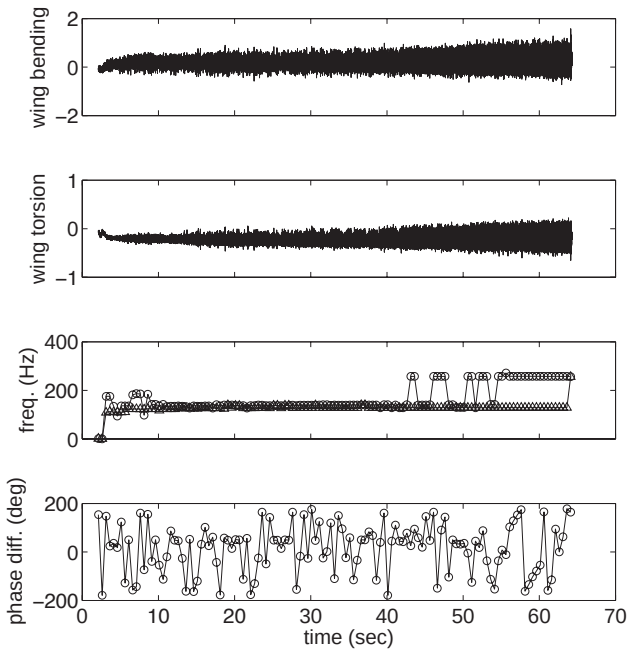

Fig. 9 Time history of strain gauge outputs, frequencies and phase difference of wing bending and torsion ($M = 0.82/P_0 = 220 - (3\,\text{kPa/s}) - 250 - (1\,\text{kPa/s}) - 300\,\text{kPa}/V = 325 - 372\,\text{m/sEAS}/\text{AoA} = +1$ degree)

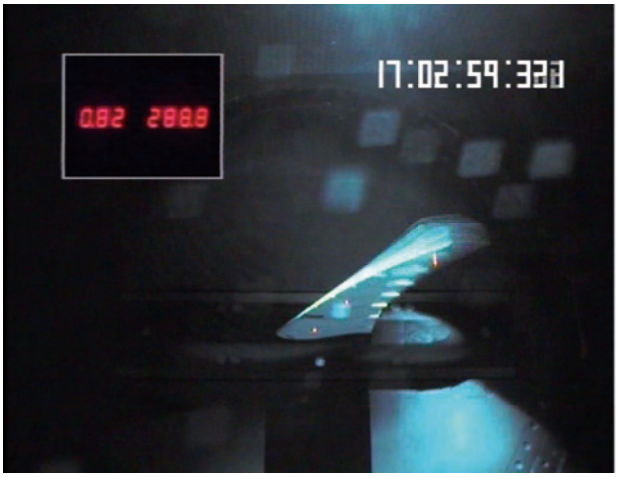

Fig. 10 Image of CCD camera (the wing without engine nacelle model)

References

[1] M. S. Hong, K. G. Bhatia, G. SenGupta, T. Kim, G. Kuruvila, W. A. Silva, R. Bartels, and R. Biedron. Simulations of a twin-engine transport flutter model in the transonic dynamics tunnel. In *Proceedings of International Forum on Aeroelasticity and Structural Dynamics 2003*, 2003.

[2] G. Dietz, H. Mai, A. Schröder, C. Klein, N. Moreaux, and P. Leconte. Unsteady wing-pylon-nacelle interference in transonic flow. In *Proceedings of 48th AIAA/ASME/ASCE/AHS/ASC Structures, Structural Dynamics, and Materials Conference*, 2007.

[3] R. Voss, M. Kreissl, J. Nitzsche, A. Soda, J. P. Grisval, and A. Dugeai. Unsteady transonic wing nacelle interference for different oscillatory motions. In *Proceedings of International Forum on Aeroelasticity and Structural Dynamics 2007*, 2007.

[4] H. Arizono, H. R. Kheirandish, J. Nakamichi, and H. Morino. Transonic flutter analysis for wing-pylon-nacelle configuration. In *Proceedings of International Forum on Aeroelasticity and Structural Dynamics 2007*, 2007.

Copyright Statement